

Short Communication

## A Novel Electrochemical Sensor for the Determination of Aflatoxin B<sub>1</sub> Based on Polymerized 4-Amino-7-azaindole-Nitrogen-Doped Graphene

Ling Shi<sup>1</sup>, Zefeng Wang<sup>1</sup>, Guangming Yang<sup>1,\*</sup>, Hongping Yang<sup>2</sup>

<sup>1</sup> Engineering Research Center for Processing and Quality Control of Local Characteristic Food and Consumer Goods of High Education in Yunnan Province, College of Science, Honghe University, Mengzi 661199, PR China

<sup>2</sup> Library, College of Science, Honghe University, Mengzi 661199, PR China

\*E-mail: [yangguangmingbs@126.com](mailto:yangguangmingbs@126.com)

Received: 4 July 2020 / Accepted: 22 July 2020 / Published: 30 September 2020

In this study, nitrogen-doped reduced graphene oxide (N-r-GO) was oxidized by HNO<sub>3</sub> to obtain porous nitrogen-doped reduced graphene oxide (P-N-r-GO). Then, it was used to drop onto the glassy carbon electrode (GCE) surface. Afterward, the above-mentioned GCE was soaked in electrolyte containing tetrabutylammonium perchlorate and 4-Amino-7-azaindole (4-NH<sub>2</sub>-7-AIH), and carried out cyclic voltammetry on the surface of P-N-r-GO and its amino group was covalently bound to the carboxyl group of AFB<sub>1</sub> antibody (Anti-AFB<sub>1</sub>). Electrochemical impedance spectroscopy (EIS) was used to monitor the electro-catalytic behavior of the modified electrodes. Under the optimized conditions, the impedance increment was linearly related to the AFB<sub>1</sub> concentration in the range of 0.025-30 ng mL<sup>-1</sup> with a detection limit of 0.006 ng mL<sup>-1</sup>.

**Keywords:** Aflatoxin; Electrochemical immunosensor; Nitrogen-doped reduced graphene oxide; Conductive polymers

### 1. INTRODUCTION

Aflatoxin B<sub>1</sub> (AFB<sub>1</sub>) is the most commonly found mycotoxins due to its highly teratogenic, hepatotoxic, oncogenic, and immunotoxic properties in human beings and animals [1-3]. The AFB<sub>1</sub> is usually existed in agricultural products such as maize, rice, peanut, grains, et al [4]. Thus, food safety becomes a very serious worldwide problem. Various countries had attached great importance for efficient analytical methods for simple, rapid and sensitive detection of AFB<sub>1</sub>.

Recently, several analytical methods have been used to detect AFB<sub>1</sub>. For example, electrochemiluminescence [1], surface-enhanced raman scattering spectroscopy [5], HPLC-MS [6],

fluorescence analysis [7] and so on. The electrochemical sensor has drawn a tremendous attention in the last decade due to easy-to-operate, portability, miniaturization and have good selectivity, sensitivity [8]. The immunosensors have received great interests due to the unique superiority of an immunoreaction with the very high sensitivity of different detectors [9]. Otherwise, the electrochemical impedance sensing possesses the advantage of simple, low-cost, relatively easy to use and have been used to detect the dynamics of bio-molecular interactions [10]. It is well known that electrochemical property can be improved by introducing nanomaterials owing to their high surface area, excellent conductivity biocompatibility, and electrocatalytic activity.

Inspired by this, we proposed an electrochemical immunosensor with the determination of AFB1. The fabrication procedure of immunosensor is illustrated in Scheme 1. Poly-4-Amino-7-azaindole (P4-NH<sub>2</sub>-7-AIH) is a good bridging agent and can functionalize P-N-r-GO. The activated AFB1 antibody is immobilized onto P4-NH<sub>2</sub>-7-AIH-P-N-r-GO through the covalent binding between its amino groups and carboxyl groups of biomolecules. The EIS technology is used to detect AFB1 with [Fe(CN)<sub>6</sub>]<sup>3-/4-</sup> as redox probe molecule.

## 2. EXPERIMENTAL

### 2.1 Apparatus and reagents

All chemicals were of analytical grade and used as received. Tetrabutylammonium perchlorate, 2-(N-Morpholino)ethanesulfonic acid, 99% and 4-Amino-7-azaindole were purchased from Beijing Balinway Technology Co. LTD. 1-Ethyl-3-(3-(dimethylamino)propyl)carbodiimide (EDC), N-hydroxysuccinimide (NHS), Aflatoxin B1 (99 %), mouse anti-AFB1 monoclonal antibody, bovine serum albumin (BSA), N-(3-dimethylaminopropyl)-N'-ethylcarbodiimide (EDC, 99%), N-Hydroxysuccinimide (NHS, 99%) were purchased from Sigma-Aldrich. Nitrogen-doped reduced graphene oxide (N-r-GO) was obtained from Nanjing Jcnano Technology Co., Ltd. The peanut sample was purchased from the local supermarket. The phosphate buffer solution (PBS, pH=7.0) was prepared with KH<sub>2</sub>PO<sub>4</sub> and Na<sub>2</sub>HPO<sub>4</sub>, and its concentration was 0.002 mol L<sup>-1</sup>.

### 2.2 Instrumentations

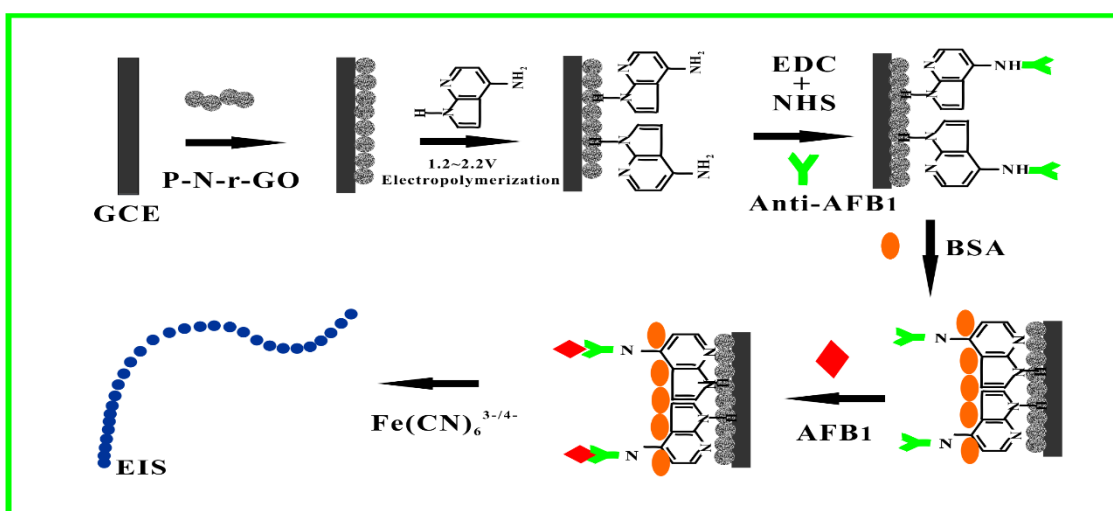
The JEM-2100 transmission electron microscope (JEOL Ltd.) and FEI Quanta 250 scanning electron microscopes was used to characterize the morphology of obtained sample. All the electrochemical experiments were carried out by an Autolab PGSTAT302N electrochemical workstation. Glass carbon electrode, saturated calomel electrode and a platinum gauze electrode were used as working, reference and auxiliary electrodes, respectively. The chromatographic analyses were carried out on Agilent 1100. The separation of the studied AFB1 was performed on a C18 (150 mm × 4.6 mm, i.d. 5.0 μm) column.

### 2.3 Preparing of porous nitrogen-doped reduced graphene oxide

The porous nitrogen-doped reduced graphene oxide (P-N-r-GO) was prepared as follows: typically, 40 mg of nitrogen-doped reduced graphene oxide (N-r-GO) was dispersed in 25 mL  $\text{HNO}_3$  solution ( $8 \text{ mol L}^{-1}$ ) via ultrasonication. The resultant mixture was refluxed for 2 h with magnetic stirring under  $100 \text{ }^\circ\text{C}$  oil bath before being cooled to room temperature. The resulting P-N-r-GO nanocomposites were collected by centrifugation, completely washed with ethanol and ultrapure water. And then the obtained products were naturally dried at room temperature for 24 h.

### 2.4 Fabrication of immunosensor

The schematic representation of fabrication process of the immunosensor was shown in Scheme 1. GCE was polished consecutively with 1.0, 0.3 and  $0.05 \mu\text{m}$   $\text{Al}_2\text{O}_3$ , followed by sonication in  $\text{HNO}_3$  ( $7 \text{ mol/L}$ ), ethanol and ultrapure water, and dried in air.  $10 \mu\text{L}$  of  $0.5 \text{ mg mL}^{-1}$  P-N-r-GO was dropped on the surface of GCE. After drying in air, the modified electrode was drenched in 4-Amino-7-azaindole ( $0.02 \text{ mol L}^{-1}$ ) containing Tetrabutylammonium perchlorate ( $0.10 \text{ mol L}^{-1}$ ) solutions. Then the polymer layer was formed on the above electrode through cycling between 1.2 V and 2.2 V for 8 cycles, and obtained poly-4-Amino-7-azaindole-P-N-r-GO modified GCE (P4-NH<sub>2</sub>-7-AIH-P-N-r-GO/GCE). On the other hand, the monoclonal antibody aflatoxin (anti-AFB1) solution ( $120 \mu\text{g mL}^{-1}$ ) was freshly prepared in phosphate buffer solution (PBS, pH 7.0). And then anti-AFB1 was activated using EDC ( $0.04 \text{ mol L}^{-1}$ ) and NHS ( $0.01 \text{ mol L}^{-1}$ ) in PBS (pH= 5.5~6.0) for 20 min. The pH value of activation solution was then adjusted to 7.2~7.8. After that, activated AFB1 antibody solution was dropped onto the P4-NH<sub>2</sub>-7-AIH-P-N-r-GO/GCE and incubated for a certain time under humid conditions at  $37 \text{ }^\circ\text{C}$ .



**Scheme 1.** Schematic representation of immunosensor fabrication.

After rinsing thoroughly with PBS (pH=7.0), the obtained electrode was then incubated in  $30 \mu\text{L}$  BSA (2.0 %) for 40 min to avoid non-specific binding of analyte onto the electrode. Finally, the

BSA-anti-AFB1-P4-NH<sub>2</sub>-7-AIH-P-N-r-GO/GCE immunosensor was washed thoroughly with PBS (pH 7.0). Next, the different concentrations of AFB1 solution was dropped onto the above electrodes and incubated for 1 h at 37 °C followed by rinsing with PBS (pH=7.0). The resulting immunosensor electrodes were applied in EIS measurement in 1.0 mmol L<sup>-1</sup> Fe(CN)<sub>6</sub><sup>3-/4-</sup>, 0.1 mol L<sup>-1</sup> KCl containing 0.002 mol L<sup>-1</sup> PBS (pH=7.0).

### 2.5 Preparation of peanut sample

The peanut was pre-treated according to the Chinese standard (GB 5009.22-2016) and the method reported by Zhang [11]. In brief, a certain amount peanut was ground to a powder. 5.0 g of power was added into centrifuge tube. Then the mixture solution of 16.8 mL acetonitrile and 3.2 mL ultra-pure water were added into centrifuge tube. The mixture solutions were vortexed and then ultrasonic 20 min. The obtained mixtures were centrifuged at 6000 rpm for 10 min. Finally, the obtained supernatant was stored at 4 °C. The obtained solution was analyzed used fabricated electrochemical immunosensor.

**Table 1.** Experimental conditions of gradient elution.

Time (min)	Water (%)	Methanol/Acetonitrile =1:1 (%)	Flow time (mL/min)
0.01	76	24	1.0
6.00	76	24	1.0
8.00	65	35	1.0
10.00	65	35	1.0
11.20	0	100	1.0
13.00	76	24	1.0

For HPLC analysis, 4.0 mL of supernatant was added into centrifuge tube and was evaporated with N<sub>2</sub> gas at 50 °C. The residue was dissolved in 200 µL n-hexane and 100 µL trifluoroacetic acid and vortexed for 30 s. The obtained solution was kept in incubator at 40 °C for deriving 15 min. Then the derivative liquid was evaporated at 50 °C with N<sub>2</sub> gas. The residue was dissolved with 1.0 mL of HPLC initial mobile phase then was vortexed for 30 s. The obtained suspension was filtered (Millipore, 0.22 µm) and the filtrate was injected to HPLC for quantitative determination of AFB1. The mobile phase was water and methanol/acetonitrile mixture solution (50+50) at a flow rate of 1.0 mL/min and gradient elute was used in all HPLC analysis. The time schedule was given in Table 1. The injection solution volume was 5 µL and column temperature was 40 °C. The AFB1 was detected by fluorescence detector and the wavelengths for excitation and emission were set at 360 nm and 440 nm, respectively. Recoveries were calculated from the average recoveries of three replicate samples.

### 3. RESULT AND DISCUSSION

#### 3.1 Characterization of as-prepared nanomaterials

TEM was used to investigate the morphology of prepared nanomaterials. Figure 1 shows the morphology and structure of the as-obtained N-r-GO and P-N-r-GO. The N-r-GO show the membrane morphology like corrugated and scrolled (Figure 1A). The P-N-r-GO exhibits a porous three-dimensional network with pore sizes of 15~25 nm (Figure 1B). The results show that multihole graphene has been successfully prepared.

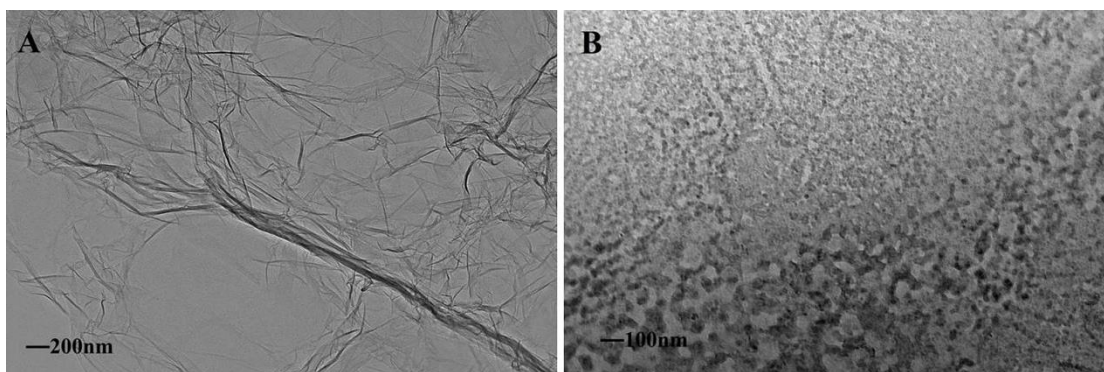


**Figure 1.** TEM images of (A) N-r-GO, and (B) P-N-r-GO

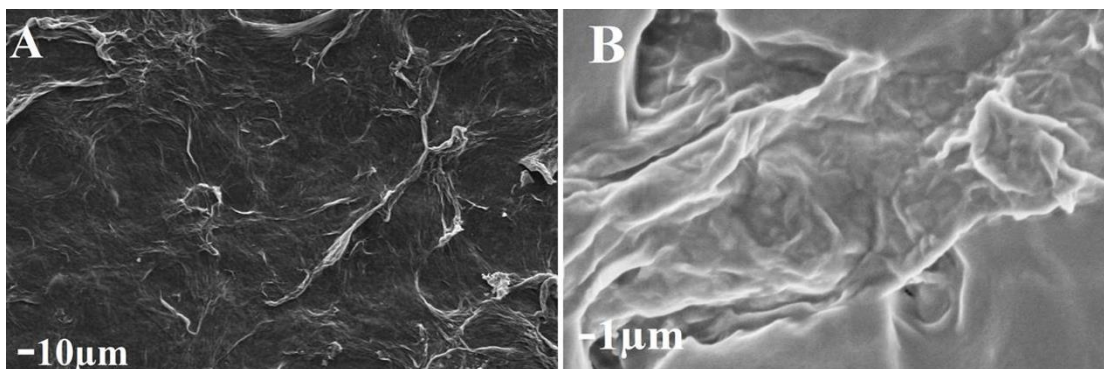


**Figure 2.** SEM images of (A) P-N-r-GO, and (B) P4-NH<sub>2</sub>-7-AIH-P-N-r-GO.

The morphologies of P-N-r-GO and P4-NH<sub>2</sub>-7-AIH-P-N-r-GO were further examined by SEM. In Figure 2A, P-N-r-GO reveals a curly morphology consisting of a thin wrinkling paperlike structure. The graphene are well-compact layer-by-layer stacking and formed layer agglomerates. When P4-NH<sub>2</sub>-7-AIH doped on P-N-r-GO surface, the obtained P4-NH<sub>2</sub>-7-AIH-P-N-r-GO reveals that the P4-NH<sub>2</sub>-7-AIH films is uniformly polymerized onto the surface of P-N-r-GO/GCE (Figure 2B). Also it reveals rather rough folded structure.

### 3.2 Characterization of the fabricated immunosensor

Figure 3 shows the EIS for each step to monitor the fabrication procedure of the immunosensor. As shown in Figure 3A, the bare GCE reveals a very small semicircle diameter (curve a), implying a diffusional limiting step of electrochemical process [12]. An almost straight line can be observed after modified with P-N-r-GO (curve b). And a straight line can be observed when modified with P4-NH<sub>2</sub>-7-AIH-P-N-r-GO (curve c). These results indicate that the P4-NH<sub>2</sub>-7-AIH-P-N-r-GO composite possesses an excellent electrochemical conductivity and is beneficial for electron transfer process. In the anti-AFB1-P4-NH<sub>2</sub>-7-AIH-P-N-r-GO modified GCE (Figure 3B, curve b), the resistance value increased obviously indicating that the modified layers hindered the access of the redox probe to the GCE surface. The resistance further increased after BSA blocking (Figure 3B, curve c). With the immunocomplex formation on the electrode (Figure 3B, curve d), the resistance increased remarkably proving that the modified layers hindered the access of the redox probe to the GCE surface. These results prove that immunosensor was successfully fabricated.

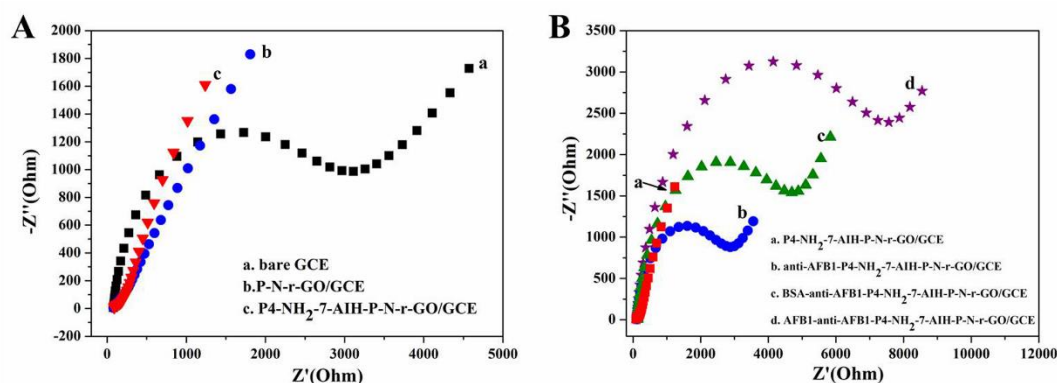


**Figure 3.** EIS of the immunosensor: A: (a) bare GCE; (b) P-N-r-GO/GCE; (c) P4-NH<sub>2</sub>-7-AIH-P-N-r-GO/GCE; B: (a) P4-NH<sub>2</sub>-7-AIH-P-N-r-GO/GCE; (b) anti-AFB1-P4-NH<sub>2</sub>-7-AIH-P-N-r-GO/GCE; (c) BSA-anti-AFB1-P4-NH<sub>2</sub>-7-AIH-P-N-r-GO/GCE; (d) AFB1-anti-AFB1-P4-NH<sub>2</sub>-7-AIH-P-N-r-GO/GCE. AFB1 concentration is 7.5 ng mL<sup>-1</sup>.

### 3.3 Optimization of immuno-assay conditions

The electrodeposition cycles of 4-NH<sub>2</sub>-7-AIH, antibody concentration, activation time, immunoreaction time, and pH value of the immunoreaction solution are great influence on the performance of immunosensor [13]. The electrodeposition cycles of 4-NH<sub>2</sub>-7-AIH on resistance value of immunosensor were investigated (Figure 4A). The resistance value increased with increasing electrodeposition cycles, suggesting gradual growth of polymeric film which covered the surface of GCE, hindering the charge transfer of the redox probe at the electrode. And a maximum resistance value was obtained when electrodeposition for 8 cycles. Hence, the optimum electrodeposition cycle was 8 cycles.

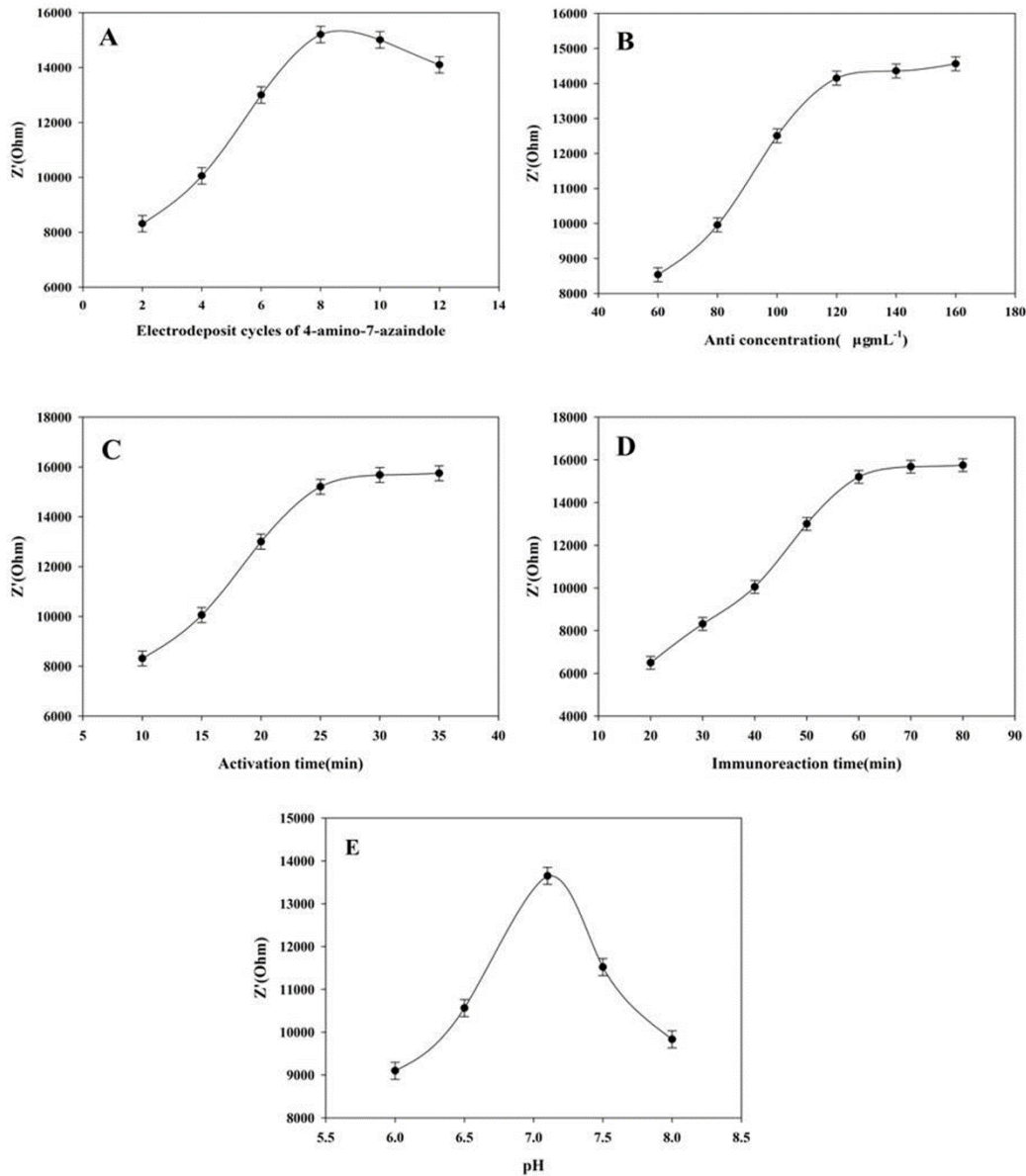


**Figure 4.** The effect of the electrodeposit cycles of 4-amino-7-azaindole (A), antibody concentration (B), activation time (C), immunoreaction time (D), and pH on resistance value of immunosensor.

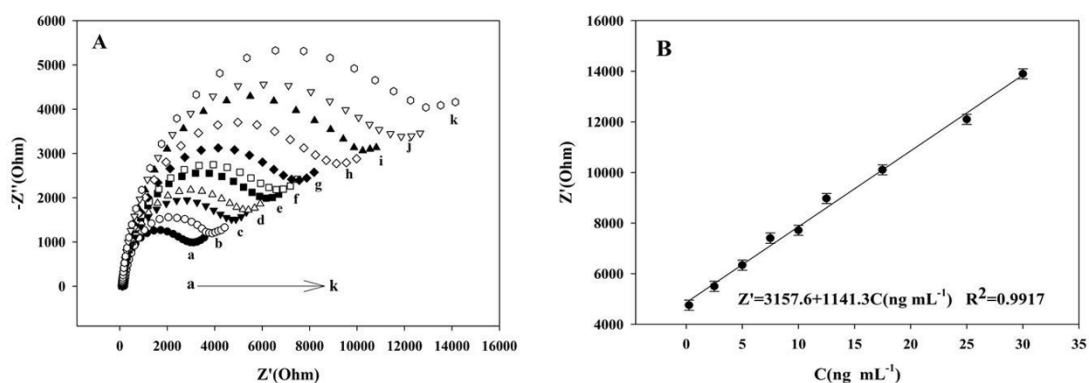
Figure 4B shows the relation between the impedance value and antibody concentration. The impedance value was significantly increased with the AFB1 antibody concentration up to 120  $\mu\text{g mL}^{-1}$  and then approximately constant due to the number of adsorptive sites was limited, saturated binding of AFB1 could be reached when antibody concentration was 120  $\mu\text{g mL}^{-1}$ . Hence, antibody concentration of 120  $\mu\text{g mL}^{-1}$  was used in follow-up experiment.

Figure 4C shows the influence of activation time of AFB1 antibody on impedance value. The impedance value increased with the activation time from 10 to 25 min and then reached to level off. Therefore, the optimal activation time was 25 min. Figure 4D reveals the influence of incubation time on impedance value. The results show that the impedance value increased with the incubation

time from 20 to 60 min and then tended to be stable. Thus, 60 min was chosen as the optimal incubation time. Figure 4E shows the effects of pH on the performance of immunosensor over a pH range from 6.0 to 8.0. The maximum impedance value was achieved at about 7.0, thus 7.0 was selected as the optimum pH value in subsequent experiments.

### 3.4 Analytical performance of immunosensor

The EIS was used to detect of AFB1 to evaluate its performance. Figure 5 reveals the impedance value responses to the specific immunointeraction on the sensing interface. As shown in Figure 5A, the impedance value increased significantly with the increase of the concentration of AFB1. A linear relation between the resistance and concentrations was observed in the range from 0.025~30 ng mL<sup>-1</sup>.



**Figure 5.** (A) Nyquist diagram of the immunosensor at different concentrations of AFB1 ranging from 0-30 (0, 0.025, 0.25, 2.5, 5.0, 7.5, 10.0, 12.5, 15.0, 20.0, 30.0) ng mL<sup>-1</sup>. (B) The linear relationship of the impedance value vs. the concentration of AFB1.

**Table 2.** Comparison between the proposed immunosensor with those reported in the literatures for AFB1 detection.

Sensor	Linear range (ng mL <sup>-1</sup> )	Limit of detection (ng mL <sup>-1</sup> )	Ref.
Reduced graphene oxide/poly(5-formylindole)/Au	0.01-100	0.002	[14]
AFB1/BSA/anti-AFB1/Au-COOH-GO	0.05-25	0.05	[15]
AFB1/Fc-apt/MCH/cDNA/AuNPs/THI-rGO/GCE	0.05-20	0.016	[16]
BSA/anti-AFB1/Au@rGO/ITO	0.10-12	0.10	[17]
This work	0.025-30	0.006	This work

The response equation was shown as  $Z' = 3057.3 + 1141.3C$  (ng mL<sup>-1</sup>),  $R^2 = 0.9917$ , and a

detection limit of  $0.006 \text{ ng mL}^{-1}$ . The detection limit was much lower than those reported in previous literatures, as illustrated in Table 2. For example, reduced graphene oxide/poly(5-formylindole)/Au ( $0.002 \text{ ng mL}^{-1}$ ) [14], AFB1/BSA/anti-AFB1/Au-COOH-GO ( $0.05 \text{ ng mL}^{-1}$ ) [15], Fc-apt-AFB1 ( $0.016 \text{ ng mL}^{-1}$ ) [16], BSA/anti-AFB1/Au@rGO/ITO [17].

### 3.5 Reproducibility, stability and selectivity of immunosensor for AFB1

The reproducibility of the EIS immunosensor was also tested by preparing three BSA-anti-AFB1-P4-NH<sub>2</sub>-7-AIH-P-N-r-GO/GCEs use same method, and used to detect  $7.5 \text{ ng mL}^{-1}$  of AFB1. The relative standard deviation (RSD) of 5.80 % was obtained by measuring the same sample with three electrodes. The results suggested the good reproducibility of this immunosensor. The stability of this immunosensor was also tested. After the immunosensor was stored at  $4 \text{ }^\circ\text{C}$  for 8 days, 96.6% (RSD=4.26 %, n=3) of the initial response was obtained, revealing the good stability of proposed sensor. The selectivity was investigated by using AFM1 and AFG1 as interfering agents. As can be seen from Figure 6, the EIS responses of blank solution, AFB1, AFG1, AFM1 were notably different. The AFG1 and AFM1 were almost no impact toward detecting AFB1. The results indicated that the satisfactory selectivity for AFB1 detection.

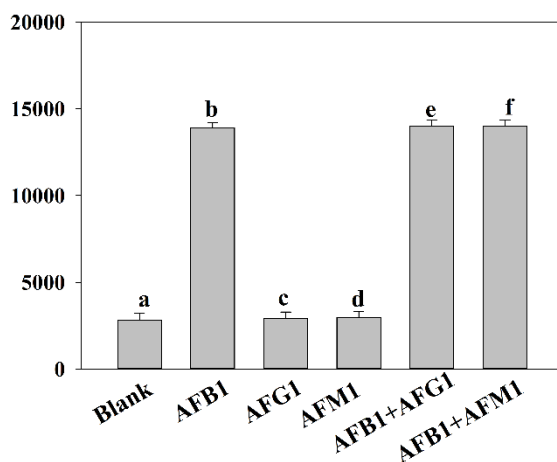


**Figure 6.** EIS responses of the immunosensor to blank sample, AFB1, AFG1, AFM1, and mixtures of AFB1 with AFG1, AFB1 with AFM1. The concentration of AFB1 is  $30 \text{ ng mL}^{-1}$ , The concentration of AFG1 and AFM1 are  $50 \text{ ng mL}^{-1}$ , n=3.

### 3.6 Analytical application

The proposed BSA-anti-AFB1-P4-NH<sub>2</sub>-7-AIH-P-N-r-GO/GCE was examined successfully for the determination of AFB1 in peanut sample. The sample was pretreated according to the method in “experiment 2.5”. The AFB1 content of peanut was  $0.28 \text{ ng mL}^{-1}$ , RSD is 3.25% (n=3). In order to further validate the feasibility of this immunosensor, high performance liquid chromatography (HPLC) method was used for peanut sample detection. The The AFB1 content of peanut was achieved of  $0.25 \text{ ng mL}^{-1}$ , which was very close to the results obtained from electrochemical analysis. Hence, the immunosensor can be practically used as a quantitative method for AFB1 detection in peanut samples.

#### 4. CONCLUSION

In this study, P4-NH<sub>2</sub>-7-AIH doped nitrogen-doped graphene was successfully deposited onto GCE surface via an electrochemical method. The obtained P4-NH<sub>2</sub>-7-AIH-P-N-r-GO nanocomposites exhibit good biocompatibility and excellent electrochemical properties. It showed fast electronic transfer kinetic, low detection limits and good stability were achieved on the as-prepared nanocomposite modified GCE. The results further revealed that the proposed sensor could be used to detect AFB1 in practical samples.

#### ACKNOWLEDGMENTS

This work was supported by the National Natural Science Foundation of China (Grand No. 21665008), Junior High School Academic and Reserve Program of Yunnan Province (Grand No. 2018HB005), Scientific Research Fundation of Yunnan Education Department (Grand No. 2020J0672), the Yunnan education department of Scientific Research Foundation (Grand No. 2018JS478), the PhD Start-up Fund of Honghe University (Grand No. XJ16B04), Young Academic Reserve Program of Honghe University (Grand No. 2016HB0401).

#### References

1. C. Sun, X. Liao, B. Jia, L. Shi, D. Zhang, R. Wang, L. Zhou and W. Kong, *Mikrochim. Acta*, 187 (2020) 236.
2. Q. Wang, Q. Yang and W. Wu, *Frontiers in microbiology*, 11 (2020) 408.
3. X. Liu, Y. Wen, W. Wang, Z. Zhao, Y. Han, K. Tang and D. Wang, *Mikrochim. Acta*, 187 (2020) 352.
4. F. Azri, R. Sukor, J. Selamat, F. Abu Bakar, N. Yusof and R. Hajian, *Toxins*, 10 (2018) 196.
5. Y. Feng, L. He, L. Wang, R. Mo, C. Zhou, P. Hong and C. Li, *Nanomaterials*, 10 (2020) 1000.
6. K. Nualkaw, S. Poapolathep, Z. Zhang, Q. Zhang, M. Giorgi, P. Li, A. Logrieco and A. Poapolathep, *Toxins*, 12 (2020) 253.
7. M. Wei, F. Zhao and Y. Xie, *Talanta*, 209 (2020) 120599.
8. E. B. Bahadır and M. K. Sezgintürk, *Talanta*, 132 (2015) 162.
9. S. Campuzano, P. Yáñez-Sedeño and J. M. Pingarrón, *TrAC, Trends Anal. Chem.*, 86 (2017) 14.
10. A. Vig, A. Radoi, X. Muñoz-Berbel, G. Gyemant and J. L. Marty, *Sensors Actuators B: Chem.*, 138 (2009) 214.
11. S. B. Zhang, Y. M. Shen, G. Y. Shen, S. Wang, G. L. Shen and R. Q. Yu, *Anal. Biochem.*, 494 (2016) 10.
12. L. Yu, Y. Zhang, C. Hu, H. Wu, Y. Yang, C. Huang and N. Jia, *Food Chem.*, 176 (2015) 22.
13. F. Arduini, I. Errico, A. Amine, L. Micheli, G. Palleschi and D. Moscone, *Anal. Chem.*, 79 (2007) 3409.
14. B. Zhang, Y. Lu, C. N. Yang, Q. F. Guo and G. M. Nie, *Biosensors Bioelectron.*, 134 (2019) 42.
15. L. Shi, Z. F. Wang, N. Wu, X. L. Chen, G. M. Yang and W. Liu, *Int. J. Electrochem. Sci.*, 15 (2020) 1655.
16. Y. Y. Li, D. Liu, Z. C. Xi, X. L. Shen, Y. Liu and T. Y. You, *J. Hazard. Mater.*, 387 (2020) 122001.
17. S. Srivastava, S. Abraham, C. Singh, M. A. Ali, A. Srivastava, G. Sumanaa and B. D. Malhotra, *RSC Adv.*, 5 (2015) 5406